

Dynamic light scattering

W. I. Goldberg

Department of Physics and Astronomy, University of Pittsburgh, Pittsburgh, Pennsylvania 15260

(Received 27 May 1999; accepted 27 July 1999)

By scattering light from small particles, their geometrical structure and their state of motion can be measured. An experiment is described for measuring the diffusivity of small particles undergoing Brownian motion using the technique called photon correlation spectroscopy or dynamic light scattering. The necessary experimental apparatus and the related theory are discussed. Photon correlation spectroscopy is a powerful tool for studying the dynamical behavior of fluids near critical points, and a discussion is given of this phenomenon. The same experimental technique also can be used to study laminar or turbulent flows, and the associated theory is introduced to enable such experiments to be interpreted. © 1999 American Association of Physics Teachers.

I. INTRODUCTION

Fractals, continuous phase transitions, spinodal decomposition, Brownian motion, the Wiener–Khinchine theorem, the Brown–Twiss effect, photon correlation spectroscopy, and turbulence. Many phenomena and ideas of great importance in statistical and condensed matter physics can be introduced by studying dynamic light scattering. The goal of this paper is to introduce this technique by describing a few experiments that can be performed by undergraduate students. The experimental possibilities are sufficiently rich that they can be stimulating to graduate students as well. The measurements require inexpensive optical components such as a small He–Ne laser (output power of a few mW), a few lenses and lens holders, and a photodetector. In addition, a more expensive device is needed, namely a photon correlator. Many correlators that may have been discarded by researchers may serve the purpose perfectly well.¹ A new correlator can be purchased for several thousand dollars.

Considerable emphasis is placed on the Brownian motion of micron-size particles diffusing in a background fluid such as water, because an understanding of Brownian motion opens the door to understanding a broad range of subjects, including the dynamical behavior of fluids and fluid mixtures, and magnetic materials near their respective critical points.

Near the critical point of fluids, we can observe fluctuations by eye and also by using a very small laser. Section II describes a desktop experiment for doing so. It turns out that these fluctuations produce the same effects as those seen in the scattering of light by small particles in Brownian motion. Readers who have only a qualitative interest in light scattering can skip directly to Sec. II. The remainder of the paper is intended for readers who are interested in setting up their own apparatus to study Brownian motion or fluid dynamics quantitatively. The same equipment can be used to make measurements in fluids near the critical point.

Suppose that the experimental components have been assembled and arranged on a table as indicated in Fig. 1. The beam of the low-power He–Ne laser is directed at a small vial or test tube filled with water in which small particles have been suspended. For the particle suspension, a drop of skim milk in water will do, but it is best to use particles, all of which have the same diameter d in the 0.01 micron to 50 micron range.² With the proper particle concentration, the sample will be pale blue when viewed in room light. A laser

beam passing through the sample should appear as a bright line which is well defined throughout the entire scattering volume.

The experimental setup in Fig. 1 shows a photodetector that collects light at a scattering angle θ equal to 90° . To satisfy the spatial coherence condition discussed below the distance R between the center of the sample cell and the photodetector should be large; say, 30–100 cm. In addition, a small pinhole of diameter h should be placed close to the photodetector face. It is helpful to mildly focus the incident laser beam on the sample volume, using, say, an $f=20$ cm lens. Ideally, the scattering particles will produce a sharply defined bright line in the fluid. Only a segment of the scattered beam should fall on the face of the photodetector. This segment can be defined by a pair of parallel closely spaced black masking tape strips placed on the sample tube (separation of the order of a mm). Alternatively, a lens can be used to form the image of the scattering volume on a slit of adjustable width L . The photodetector then accepts light from scattering particles within the segment. Spatial coherence is achieved by choosing h , L , and R to satisfy the condition

$$B = hL/R\lambda \lesssim 1. \quad (1)$$

where λ is the wavelength of light in the water sample of refractive index n , and λ is related to the vacuum wavelength of the laser beam λ_{vac} by $\lambda = \lambda_{\text{vac}}/n$. For water $n = 1.3$.³ The optical coherence condition in Eq. (1) is familiar from elementary optics. When Eq. (1) is satisfied, the photodetector collects light from only the first diffraction maximum produced by a slit of width L . For studies of Brownian motion, one might want to choose L , R , and h so that B is less than 10 or so (for studies of fluid motion discussed in Sec. IV, B should be less than unity).

The photodetector should be operated as a pulse counting device rather than in an analog mode, that is, it should sense the individual photoelectron pulses. The width of these pulses is not relevant to the experiment; only their spacing in time is important. It is preferable if all the photopulses are of the same width and amplitude, which is accomplished by passing the photodetector output through a discriminator. The individual pulses coming out of the discriminator should be less than $1 \mu\text{s}$ in width and ideally less than $0.1 \mu\text{s}$. Many photodetectors come with a built-in discriminator with a TTL output.

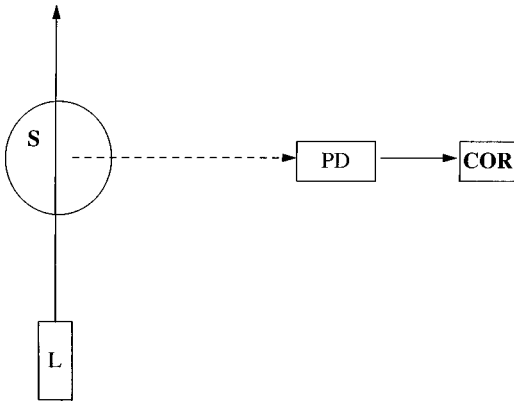


Fig. 1. Experimental setup for studying the Brownian motion of particles in water. The sample is labeled *S*. The laser *L* directs the incident beam vertically upward. The photodetector PD converts the scattered light into a pulse string which is fed to the correlator COR.

To be sure that all the optics and electronics are arranged correctly, it is useful to observe the chain of TTL pulses on an oscilloscope before sending them to the correlator. If the TTL pulse width is shorter than $0.1 \mu\text{s}$, use very short interconnecting cables or be sure that all outputs and inputs are terminated in the characteristic impedance of the cable, which is 50Ω for RG58U cable. This is to avoid reflection of pulses from the ends of the cable due to impedance mismatching problems. Data collection will be tedious if the mean photon counting rate $\langle I \rangle$ is less than 1000 counts/s.

Figure 2(a) shows a chain of photodetector pulses produced by incoherent light falling on the photodetector. The pulses occur at random times, with their mean spacing being inversely proportional to $\langle I \rangle$. Figure 2(b) shows the detector output from light that is scattered by diffusing particles in the sample. In both experiments the photon pulses have passed through a discriminator, assuring that all the pulses have the same height and width. In Fig. 2(b) the pulses are correlated in time, that is, they are bunched together within a correlation time τ_c which is determined by the diffusion coefficient of the particles and the scattering angle. The photon correlator identifies this clustering effect by measuring the correlation function

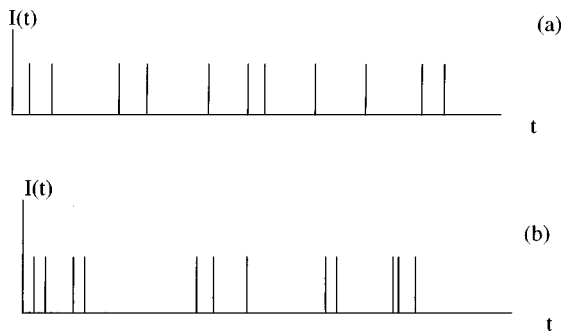


Fig. 2. (a) The output of the PD for immobile scatterers, as might be the case if the sample has been frozen or if the sample is a piece of milk glass or even a piece of paper. The arrival time of the photopulses is purely random in this case. (b) The PD output of moving particles which are Doppler shifting the frequency of the incident light. Note that the pulses tend to cluster in time. This clustering time or correlation time τ_c is inversely proportional to the diffusivity of the randomly moving particles that scatter the light.

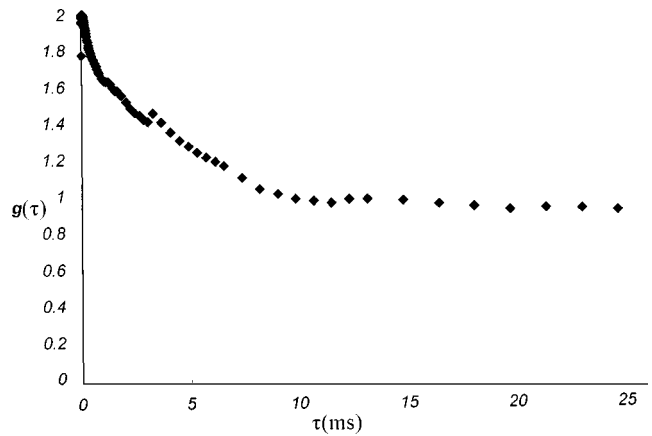


Fig. 3. Plot of $g(\tau)$ versus τ measured in a soap film which was only a few μm thick. The soap solution was a 1% dish washing detergent in water. The seed particles were polystyrene spheres of diameter 1μ . Note that $g(0) \approx 2$.

$$K(\tau) = \langle I(t)I(t+\tau) \rangle \quad (2)$$

or its dimensionless counterpart

$$g(\tau) = \langle I(t)I(t+\tau) \rangle / \langle I(t) \rangle^2. \quad (3)$$

Experimentally, the average designated by the brackets in Eq. (3) is a time average over the data collection interval T :

$$K(\tau) = \frac{1}{T} \int_0^T I(t)I(t+\tau) dt, \quad (4)$$

where T typically ranges from seconds to many minutes, with the choice dictated by the desired signal-to-noise ratio. The mean intensity is the time average, $\langle I \rangle = (1/T) \int_0^T I(t) dt$.

In the experiments discussed here, the system is in thermal equilibrium, or as in Sec. V, in a stationary state. In either case $\langle I(t) \rangle = \langle I(t+\tau) \rangle$, a fact that will be invoked repeatedly. Of course, $K(\tau)$ is *not* independent of τ ; its τ -dependence is what we are interested in measuring and calculating. Its characteristic decay time will be denoted as τ_c . Typically τ_c is in the range of hundreds of microseconds to milliseconds, depending on the particle size used.

The signal-to-noise ratio, S/N , will always improve if the data collection time T is increased. Suppose that we are content with data for which $g(\tau)$ is measured within 1%. First assume that the counting rate $\langle I \rangle$ is so large that the quality of the measurements is not determined by the low counting rate, but is limited by the number $N_c = T/\tau_c$, of “fluctuations” collected in the time T . According to Poisson statistics,⁴ $S/N = 1/\sqrt{N_c}$, and hence, one percent accuracy is achieved by setting $T/\tau_c = 10^4$.

Next consider the opposite limit where the scattered intensity $\langle I \rangle$ is very low. In this limit, the fluctuations in $g(\tau)$ will be governed by so-called shot noise and will vary as the inverse square root of the measuring time T . In this low counting rate limit, where Poisson statistics is again relevant, T/τ_c is no longer the controlling parameter; to make a measurement to 1% accuracy, choose $T\langle I \rangle = 10^4$.

Figure 3 shows a measured $g(\tau)$ produced by small particles in Brownian motion. The solution in which they are

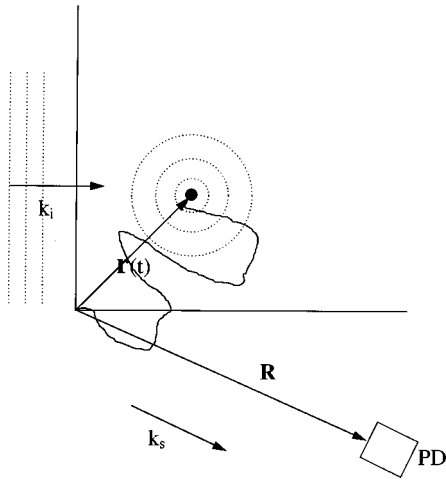


Fig. 4. Sketch of diffusing particle with an incident beam traveling from left to right. The particle is located at the origin of the coordinate system at time $t=0$ and at time t its position is $\mathbf{r}(t)$. The photodetector is labeled PD. The directions of the incident and scattered beams are shown.

moving is a soap film only a few μm thick. For spherical Brownian particles diffusing in the background solvent, it can be shown⁴ that the function

$$G(\tau) \equiv g(\tau) - 1 \quad (5)$$

decays exponentially, with the decay rate given by

$$\tau_c^{-1} = 2Dq^2. \quad (6)$$

Here D is the diffusion coefficient of the particles and \mathbf{q} is the scattering wavevector whose magnitude q is given by

$$q = |\mathbf{q}| = \frac{4\pi}{\lambda} \sin \frac{\theta}{2}, \quad (7)$$

where θ is the scattering angle and λ is λ_{vac}/n .

In a time t a particle will diffuse a mean square distance $\langle r^2 \rangle$ that is proportional to Dt . The diffusion produces a large fluctuation in the intensity in a time t' such that $t' \approx 1/(Dq^2)$. This characteristic time t' is of the order τ_c . It is these intensity fluctuations that a photon correlator measures. Helpful discussions of diffusion can be found in Refs. 4 and 5.

The diffusion coefficient D depends on the particle diameter d . For spherical particles, $D = k_B T / 3\pi\eta d$,⁶ where T is the temperature, k_B is Boltzmann's constant, and η is the viscosity of the background fluid. From this relation, we have $\eta = 0.01 \text{ g cm}^{-1} \text{ s}^{-1}$ and $D = 4.4 \times 10^{-9} \text{ cm}^2/\text{s}$ for a diffusing particle $1 \mu\text{m}$ in diameter in water at room temperature. From a measurement of $g(\tau)$, we can obtain τ_c^{-1} and find the radius of the diffusing particles, even if they are too small to be observed with a microscope. (See Fig. 4.) Similarly, a measurement of $g(\tau)$ enables us to measure the radius of gyration of polymer molecules diffusing in solution and to determine the correlation length of fluctuations in density or concentration in a fluid or mixture near its critical point.^{7,8} Measurements of $g(\tau)$ can be a powerful tool for studying phenomena that have nothing to do with diffusion, for example, the determination of the width of a narrow spectral line⁹ or the diameter of a distant double star.¹⁰ The latter experiment gave birth to the technique of photon correlation spectroscopy.

All photodetectors generate output pulses even when there is no light shining on them. This dark count rate can be a few Hz to several kHz. Except at very small τ , these dark count pulses occur roughly randomly in time and hence give a flat background to $g(\tau)$, reducing the relative contribution of $G(\tau)$, the quantity in which we are really interested. In room light the photodetector will have the same effect. It is therefore necessary to employ a laser-generated counting rate that is many times larger than the dark count rate and room light count rate, in addition to satisfying the condition $\langle I \rangle \tau_c \gg 1$. The contribution to $\langle I \rangle$ from room light can be reduced by placing an inexpensive interference filter¹¹ directly in front of the photodetector and interposing a tube between it and the sample. A cardboard tube works well. For the most noise-free results, turn off the room lights when the correlator is making measurements.

If a flowing fluid is seeded with small particles, we can learn a lot about the flow by measuring $g(\tau)$. The fluid flow problem is treated in Sec. V. It will be seen that $g(\tau)$ gives information about velocity differences between pairs of points in the flow. Laminar and turbulent flows can be studied in the laboratory¹²⁻¹⁴ using the same apparatus as that employed in the Brownian motion measurements.

In Sec. III the intensity correlation function is calculated for a single Brownian particle, with the assumption that the photodetector is so small that the scattering wave vector \mathbf{q} is sharply defined. The calculation will be valid even when many particles are present in the sample, as long as they are sufficiently far apart that they do not interact. We will see that when B is no longer very small, $G(\tau)$ is diminished by a factor $f(A)$ which takes into account the fact that photons scattered from the most widely separated diffusing particles in the sample will interfere with each other to give

$$G(\tau) = g(\tau) - 1 = f(A)e^{-2Dq^2\tau}. \quad (8)$$

The argument A in $f(A)$ is the area of the photodetector, an important parameter in the subsequent calculation of $f(A)$ in Sec. IV.

The single-particle calculation of $g(\tau)$ is presented in Sec. III. To find $f(A)$ in Eq. (8), we must consider the motion of many Brownian particles, because its attenuating effect arises from the interference of the electric fields scattered by these particles. The calculation of $f(A)$ appears in Sec. IV.

The basic theory developed in Secs. II and III can be applied with little modification to the study of laminar and turbulent flows, which is the subject of Sec. V. Some concluding remarks are given in Sec. VI.

II. CRITICAL PHENOMENA, LIGHT SCATTERING, AND BROWNIAN MOTION

Light scattering is a very powerful tool for studying critical phenomena. Some of the central features of continuous phase transitions are easily observed and can be presented in a lecture demonstration or observed on a desktop.

Here we briefly review the subject of critical phenomena and describe an experiment for observing a striking manifestation of it, namely critical opalescence. You can observe this effect with a very small laser of the type used as a pointer in lecture halls. In addition, you will need a small glass container to hold the sample, which might be a mixture of 2,6-lutidine and water (LW), available from a chemical supply house. A convenient sample cell is a vial of diameter

≈ 1 cm and a height of several centimeters. The vial should have a good screw top, because 2,6-lutidine¹⁵ has a very unpleasant smell. The trick is to prepare the LW mixture so that the lutidine concentration c is close to the critical concentration, c_c , which is 28% by weight. In a binary mixture such as LW, the concentration variable plays the same role as the density in a simple fluid such as water or CO₂.¹⁶

Sample preparation should be carried out under a hood or in a very well ventilated space. After the water and lutidine have been placed in the container with its composition within a few percent of c_c and shaken up, it will be in one phase if the temperature is less than the critical temperature, $T_c = 33.4^\circ\text{C}$. Place the cell in a beaker of water, which will serve as a temperature bath. The bath is then heated by adding hot tap water. When the sample is held for a few minutes at a high temperature well above T_c , it will separate into two well-defined phases, with the heavier water-rich phase on the bottom.

If you were successful in preparing a sample close to the critical concentration, the volumes of the two phases will be almost equal. If not, insert a syringe into the cell and draw out the excess phase (or add a drop or two of the appropriate minority component), so that the two phases have equal volume. After this single iteration, you have probably prepared the mixture adequately close to T_c .

To observe critical opalescence, return the sample cell to the water bath and heat it slowly, shaking the sample cell now and then to bring the mixture to the same temperature as that of the surrounding bath. When T is increased through T_c from below, droplets will form, and after several minutes, the more dense water-rich phase will settle to the bottom and two sharply defined phases will be seen. The most instructive observations are made when the system is still in one phase, so increase the bath temperature slowly as T_c is approached.

When the temperature becomes close to T_c , the sample will develop a brownish appearance because it is strongly scattering the room light. The scattering may become so large that the laser beam, which you should now be sending through the sample, may hardly go through it. This phenomenon is called critical opalescence. Place a sheet of paper so that you can view the transmitted beam. You should see that the scattered light consists of speckles that flash on and off in a random fashion.

How are we to understand this strong scattering phenomenon when the system is in one phase but close to T_c ? Near the critical point, small regions of water rich and lutidine rich phases momentarily form and then diffuse away. This same phenomenon occurs far from the critical point, but the size of the regions is much smaller than the wavelength of light, and the regions come and go so quickly that most measuring instruments will not be able to record them. Similarly, a glass of water near room temperature undergoes fluctuations in density, but these fluctuations are so small in spatial extent and in amplitude that they cannot be easily observed. Moreover, the fluctuation rate Γ is very fast far above or below T_c , because small-scale density variations diffuse away faster than large ones, making them unobservable by eye and even by very fast electronic equipment.

Near the critical point, the free energies of the one-phase states and the two-phase states are almost the same. As a result, the system makes brief excursions or fluctuations from the one-phase state to the two phase state, that is, it locally tries to phase separate, even though the system is

globally in one phase. These local fluctuations in density or composition produce local variations in the refractive index n . It is these local variations in n that scatter the light, just as a small lens would. As T_c is approached, these composition fluctuations grow in magnitude and in spatial extent ξ and can become even larger than the wavelength of light. The fluctuations of size ξ cause $G(\tau) = g(\tau) - 1$ to vary as $e^{-2Dq^2\tau}$, just as for Brownian particles (provided $q\xi < 1$). The diffusivity D in $G(\tau)$ is the same as that of a Brownian particle, except that the radius $d/2$ of the diffusing particle is replaced by ξ .

The reader interested in learning more about critical phenomena and the role of light scattering has many sources of information available, such as those collected in Refs. 8, 16, and 17.

III. INTENSITY CORRELATION FUNCTION FOR BROWNIAN PARTICLES

We first deduce the limiting value of $g(\tau)$ for $\tau \gg \tau_c$. In this limit the intensities at t and $t + \tau$ are unrelated, so $K(\tau) = \langle I(t) \rangle \langle I(t + \tau) \rangle \rightarrow \langle I(t) \rangle^2 = \langle I(t + \tau) \rangle^2$ in steady or equilibrium states. Therefore $g(\tau \rightarrow \infty) = 1$ in Eq. (3).

In the opposite limit $\tau \ll \tau_c$, the scattered intensities at the times t and $t + \tau$ are almost equal, so that $g(\tau) \rightarrow \langle I^2 \rangle / \langle I \rangle^2$, which is in general greater than unity. For the Brownian motion problem, we will see that $g(\tau \rightarrow 0) = 2$. If the sample contains large specks of dust that produce occasional bright flashes of light when floating through the laser beam, we are no longer dealing with the Gaussian statistics of Brownian motion, and $g(0)$ can greatly exceed two.

We are interested in $g(\tau)$ generated by non-interacting Brownian particles such as polystyrene latex spheres of diameter $d = 1 \mu\text{m}$ in a small container of water. As a starting point, consider a particular particle located at $\mathbf{r}(t)$ at time t that was at $\mathbf{r}(0)$ at $t = 0$. A laser beam traveling along the y axis illuminates the particle, which then scatters the incident beam. The photodetector, which is located a large distance R from the origin, senses the scattered field, producing photo-pulses at the (fluctuating) counting rate $I(t)$. The intensity $I(t)$ is proportional to the square of the incident electric field E_i , which is assumed to be of complex form:

$$E_i = \mathcal{E}_0 e^{-i\mathbf{k}_i \cdot \mathbf{r}(t_0) + i\omega t_0}, \quad (9)$$

where ω is an optical frequency of the order of 10^{15} Hz and t_0 is the instant when the scattered wave leaves the particle. Here \mathbf{k}_i has the direction of the incident beam and its magnitude is $k_0 = 2\pi/\lambda$. Because we are ultimately interested in the ratio of scattered intensities, nothing is lost by taking this field to be expressed in dimensionless units. The scattered field E_s is a spherical wave whose amplitude is proportional to the incident field amplitude:

$$E_s(\mathbf{R}, t) \propto \frac{E_i(t_0) e^{-ik_0|\mathbf{R} - \mathbf{r}(t_0)|}}{|\mathbf{R} - \mathbf{r}(t_0)|} e^{i\omega(t - t_0)}. \quad (10)$$

The intensity is

$$I(t) = \text{Const } E_s(\mathbf{R}, t) E_s^*(\mathbf{R}, t). \quad (11)$$

The constant of proportionality depends on many parameters, including \mathcal{E}_0 and R . The factor $e^{i\omega t}$ in Eq. (10) will sometimes be suppressed because it will always be canceled

out for any measurable quantity. The units of the electric field will be chosen such that $E_s(t)E_s^*(t) = I(t)$. In the next section, quantities like K and Q (the analog of \tilde{Q}) will have different units, but the quantities of interest, namely $g(\tau)$ and $f(A)$, will remain dimensionless.

Equation (10) can be simplified by taking advantage of the fact that $|\mathbf{R}|$ is much greater than $|\mathbf{r}(t)|$ in all cases of experimental interest. Then the exponent in Eq. (10) can be expanded to give the phase factor

$$\begin{aligned}\Delta\phi(t) &= k_0|\mathbf{R} - \mathbf{r}(t_0)| \\ &= k_0\sqrt{R^2 - 2\mathbf{R}\cdot\mathbf{r} + r(t_0)^2} \simeq k_0R - k_0\mathbf{R}\cdot\mathbf{r}(t_0)/R.\end{aligned}$$

We define the scattered light wave vector $\mathbf{k}_s = k_0\mathbf{R}/R$, so that, to a good approximation, $\Delta\phi = k_0R - \mathbf{k}_s\cdot\mathbf{r}(t_0)$. Defining

$$\mathbf{q} = \mathbf{k}_s - \mathbf{k}_i, \quad (12)$$

we can write the total scattered field at time t produced by the Brownian particle as

$$E_s(t) \propto \frac{e^{-i\mathbf{q}\cdot\mathbf{r}(t_0) + i\omega t}}{R},$$

where we have dropped the \mathbf{r} -independent factor e^{ik_0R} . In addition, the denominator is approximated by R , because in all experiments $R \gg r$. The vectors appearing here are shown in Fig. 4.

Because the flight time of the photon, $t - t_0$ is very short (much shorter than the time for a particle to diffuse an optical wavelength), t_0 can be replaced by t , so that the above equation, combined with Eq. (9), can be written

$$E_s(t) \propto \frac{e^{-i\mathbf{q}\cdot\mathbf{r}(t) + i\omega t}}{R}. \quad (13)$$

The scattering of photons by the small particles is almost perfectly elastic, so that the magnitude of the incident and scattered photons is equal, $|\mathbf{k}_s| = |\mathbf{k}_i| = 2\pi/\lambda \equiv k_0$. If the scattering angle is θ , then $q = 2k_0 \sin(\theta/2)$. This result is quickly obtained from a sketch of the two vectors \mathbf{k}_s and \mathbf{k}_i drawn so that their tails touch each other, with the angle θ between them. As expected, when θ is zero and π , q is zero and $2k_0$, respectively.

In this discussion, the vector nature of the electric field has been ignored, so polarization effects were not considered. Such effects are not important if the refractive index of the scattering particle is close to that of the surrounding fluid.¹⁸ If this condition is fulfilled, the scattered light will have the same polarization as that of the incident beam, because the scattering particles behave almost like point dipoles, their dipole moment being induced by the incident electric field.¹⁹

The above derivation is for an ensemble of non-interacting Brownian particles, a condition that is well fulfilled if the particle density is low enough that the beam traces a sharp line through the fluid. In the limit of extreme multiple scattering, \mathbf{k}_s would no longer be well-defined, and the scattering wave vector $\mathbf{q} = \mathbf{k}_s - \mathbf{k}_i$ would have lost its meaning.

In a macroscopic time interval t , the distance $\mathbf{r}(t)$ traversed by a Brownian particle is a Gaussian random variable; its position in a liquid is the sum of many independent steps of atomic size. According to the central limit theorem,⁵ a random variable $\mathbf{r} = \sum \delta\mathbf{r}_i$ which is the sum of a very large

number of independent random variables $\delta\mathbf{r}_i$, has a Gaussian distribution, regardless of the functional form of the distribution of the individual terms. In three dimensions²⁰

$$P(r) = (4\pi Dt)^{-3/2} e^{-r^2/4Dt}. \quad (14)$$

This probability density function describes the position distribution of a large assembly (or ensemble) of particles initially located at $\mathbf{r} = 0$ at $t = 0$. The integral of P over all space is unity at $t = 0$ and at all subsequent times. According to Eq. (14), P is an infinitely sharp spike or delta function at $t = 0$. As time progresses, P broadens, but its maximum does not shift. This broadening of $P(t)$ describes the diffusion of an ink drop that is initially infinitely small and subsequently spreads out as a spherically symmetric cloud, fading at its edges. Of course, ink particles are Brownian particles themselves, rendered observable by their color.

We now turn our attention to a calculation of the electric field correlation function $g_1(\tau)$, a complex quantity defined as

$$\begin{aligned}g_1(\tau) &\equiv \langle E_s^*(t)E_s(t+\tau) \rangle / \langle I \rangle \\ &= \langle e^{i\mathbf{q}\cdot\mathbf{r}(\tau)} \rangle e^{i\omega\tau} = \int P(r) e^{i\mathbf{q}\cdot\mathbf{r}} d^3r e^{i\omega\tau},\end{aligned} \quad (15)$$

so that

$$\begin{aligned}g_1(\tau) &= (4\pi D\tau)^{-3/2} e^{i\omega\tau} \int_{-\infty}^{\infty} e^{-r^2/2D\tau} e^{-i\mathbf{q}\cdot\mathbf{r}} d^3r \\ &= e^{-Dq^2\tau} e^{i\omega\tau}.\end{aligned} \quad (16)$$

Written out in full, $K(\tau)$ in Eq. (2) is

$$K(\tau) = \langle E_s^*(t)E_s(t)E_s^*(t+\tau)E_s(t+\tau) \rangle. \quad (17)$$

The motion of a single particle will Doppler shift the frequency of plane waves falling upon it, but a photodetector will not record a fluctuation in the total scattered intensity $E_s(t)E_s^*(t)$, since the time-dependent phase factors in $E_s(t)$ and $E_s^*(t)$ cancel. To observe intensity fluctuations in a photodetector, one must have at least two particles present, so that their relative motion will generate a beating of the scattered electric fields. It turns out, as one will see, that the only terms contributing to $g(t)$ are such pairwise terms.

We are interested in $g(\tau) = \langle I(t)I(t+\tau) \rangle / \langle I \rangle^2$, when the sample consists of a very large number N of particles exposed to the incident plane wave. Writing out the numerator and denominator of $g(\tau)$ in full and dropping the subscript ‘‘s,’’

$$\begin{aligned}g(\tau) &= K(\tau) / \tilde{Q}^2 \\ &= \sum_{i,j,k,l} \langle E_i(t)E_j^*(t)E_k(t+\tau)E_l^*(t+\tau) \rangle / \tilde{Q}^2,\end{aligned} \quad (18)$$

where

$$\langle \tilde{Q}(t) \rangle = \langle I(t) \rangle = \sum_{i,j} E_0^2 \langle e^{i(\mathbf{q}\cdot\mathbf{r}_i(t))} e^{-i(\mathbf{q}\cdot\mathbf{r}_j(t))} \rangle.$$

There are N^4 terms in K and in \tilde{Q}^2 , but in the ensemble averaging operation, most of them are zero because they correspond to fluctuations at optical frequencies or because the particles are, by assumption, uncorrelated in their motion. (See the next section for more details.) The only surviving

terms are those for which $i=l$ and $j=k$. The absence of a correlation between the particles enables one to factor functions like $\langle E_i(t)E_i^*(t+\tau)E_j^*(t)E_k(t+\tau) \rangle$ into the product of pairwise correlation functions with $i=l$ and $j=k$, so that this product may be written $\langle E_i(t)E_i^*(t+\tau) \rangle \langle E_j^*(t)E_j(t+\tau) \rangle$ with $i \neq j$. Because all particles scatter identically, this term has the same value as $|\langle E_i(t)E_i^*(t+\tau) \rangle|^2$, even though it represents a beating term between different particles i and j . There will be $N^2 - N \approx N^2$ such electric field correlation function terms in $K(\tau)$.

Now consider those terms for which $i=j$ and $k=l$, namely $\sum_{i,j} \langle E_i(t)E_i^*(t)E_j(t+\tau)E_j^*(t+\tau) \rangle$. It is equal to $N^2 E_0^2 = \langle I \rangle^2$, or equivalently $N^2 |\langle E(t) \rangle|^2$, where E is the field scattered by a single particle.

Collecting these results and putting them in Eq. (15) permits one to write

$$g(\tau) = 1 + \frac{|\langle (E(t)E^*(t+\tau)) \rangle|^2}{|\langle E(t) \rangle|^2}. \quad (19)$$

Or equivalently,

$$g(\tau) = 1 + |g_1(\tau)|^2. \quad (20)$$

The correlation function is written in the above way because the result holds more generally than suggested by this derivation; Eq. (20) is valid for any N -particle system, as long as the total scattered field, $E_s = \sum_j E_j$ is a (two-dimensional) Gaussian random variable. This important equation is called the Bloch–Siebert theorem. Its full derivation can be found in Ref. 21.

Because $\langle |E^*(t)E(t+\tau)| \rangle / \langle |E(t)|^2 \rangle = e^{-2Dq^2\tau}$, we have,

$$g(\tau) = 1 + e^{-2Dq^2\tau}, \quad (21)$$

which is our central result.

Equation (21) gives the correct τ dependence of $G(\tau) = g(\tau) - 1$, even when B is large and $f(A)$ in Eq. (8) is correspondingly small. On the other hand, it fails when applied to flowing fluids, where the particles are no longer moving independently. In that case, the factorization of the fourfold correlation function in $K(\tau)$ is no longer permissible, and one must turn to the formalism presented in Sec. V.

For a sample containing a spread of particle diameters, such as dilute milk, $g(\tau)$ will consist of a sum or integral of exponentially decaying contributions of the form $e^{-2D_j(d)q^2\tau}$, with each term appropriately weighted by a concentration factor $c_j(d)$. There exists a large body of literature dealing with this weighting problem, as it is of great practical importance.²² Further complications arise if the Brownian particles are not spherical in shape.⁷

So far we have considered only the limit $B \ll 1$, so that the photodetector is receiving light from a single scattering vector, \mathbf{k}_s . That restriction is lifted in the next section. In many experiments, the finite area of the photodetector changes only the amplitude of $G(t)$, but for fluid flow, the shape of this function can be appreciably changed if B is not less than unity.^{12,13}

IV. THE EFFECT OF SPATIAL INCOHERENCE

The goal of this section is to calculate the (de)coherence factor $f(A)$ in Eq. (8). This function will depend on the precise shape and size of the source as seen by the photode-

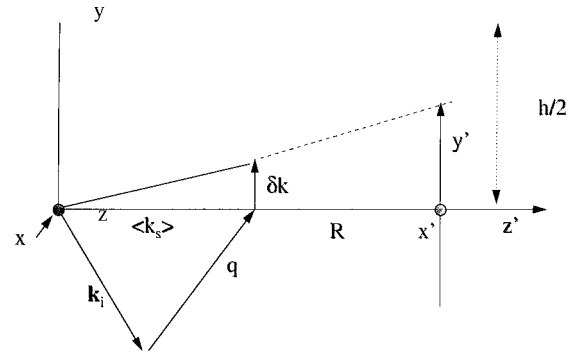


Fig. 5. Schematic diagram showing the scattering geometry and the coordinate directions discussed in Sec. IV. The incident beam \mathbf{k}_i , like all the other wave vectors shown, lies in the plane of the paper. The scattering wave vector (or the momentum transfer) for the photon striking the photodetector surface at the point $(x'=0, y'=0)$ is $\Delta\mathbf{k} = \mathbf{k}_s - \mathbf{k}_i = \mathbf{q} + \delta\mathbf{k}$. Here \mathbf{q} is the average value of $\Delta\mathbf{k}$. In the detailed calculations presented here, the incident beam is travelling in the $-y$ direction, and the photodetector is a square of area $h \times h$ or a circle of diameter h . A second coordinate system x', y', z' is at the geometrical center of the photodetector.

tor and on the same parameters for the photodetector surface with area A . Consider the special geometrical arrangement shown in Fig. 5. The wave number \mathbf{k}_i of the incident laser beam has been chosen to lie in the plane of the paper, and the photodetector receives light from a range of \mathbf{k}_s values. The mean value of the scattered wavevector $\langle \mathbf{k}_s \rangle$ points along the z axis in Fig. 5, so the average scattering vector \mathbf{q} is given by $\mathbf{q} = \langle \mathbf{k}_s \rangle - \mathbf{k}_i$. Its direction and magnitude are shown in Fig. 5.

The rectangular coordinate system is centered at a point near the center of the sample. Another coordinate system x', y', z' is also employed. The origin of this coordinate system is at the geometrical center of the photodetector; its face is assumed to be square, with dimensions h . If the photosensitive area is circular, its radius is also taken to be h .

The detector collects light from a range of scattered vectors \mathbf{k}_s , and the photon momentum transfer is designated as

$$\Delta\mathbf{k} = \mathbf{k}_s - \mathbf{k}_i = \mathbf{q} + \delta\mathbf{k}. \quad (22)$$

For the j th particle the scattered electric field is

$$E_j = E_0 e^{-i\Delta\mathbf{k} \cdot \mathbf{r}_j(t) + i\omega t}. \quad (23)$$

The subscript ‘‘s’’ in the scattered field has now been dropped. It will be assumed, as before, that all scattering particles have the same diameter, so that the scattering amplitude E_0 is common to all of them. Therefore it does not appear in $g(\tau)$, and we set it equal to unity.

The correlation function $K(\tau)$ in Eq. (8) is the product of four electric field factors, each of which is now a sum over all N particles in the sample. The scattered photons will go to all points on the face of the photodetector, and for each point, the momentum transfer $\Delta\mathbf{k}$ will be different. We need to sum over all such points or rather integrate over the photosensitive area A .

At time t , the product $E_i(t)E_j^*(t)$ will contain terms such as $e^{i(\mathbf{q} + \delta\mathbf{k}) \cdot (\mathbf{r}_j(t) - \mathbf{r}_i(t))}$, where we have replaced $\Delta\mathbf{k}$ by its equivalent, $\mathbf{q} + \delta\mathbf{k}$. In writing this expression, it has been recognized that to a very good approximation $\mathbf{q} + \delta\mathbf{k}$ is inde-

pendent of the particle positions $\mathbf{r}_n(t)$, so this momentum change is independent of particle position in the sample.

The notation is simplified by letting $\mathbf{r}_{ij} = \mathbf{r}_j(t) - \mathbf{r}_i(t)$. In the short time interval τ , particles i and j change their relative positions by a distance $\delta\mathbf{r}_{ij}(\tau)$, so at time $t + \tau$, the difference in positions of this particle pair is $\mathbf{r}_{ij}(t) + \delta\mathbf{r}_{ij}$. Integrating the scattered intensity over the area of the photodetector for both $I(t)$ and $I(t + \tau)$, we obtain

$$g(\tau) = K(\tau)/Q^2 = \left\langle \int_A I(t) dA' \int_A I(t + \tau) dA' \right\rangle / Q^2, \quad (24)$$

where

$$\begin{aligned} Q(t) &= \left\langle \int_A I(t) dA' \right\rangle = \left\langle \sum_{i,j} \int_A e^{i(\mathbf{q} + \delta\mathbf{k}) \cdot \mathbf{r}_{ij}(t)} dA' \right\rangle \\ &= \sum_{i,j} \left\langle \int_A e^{i(\mathbf{q} + \delta\mathbf{k}) \cdot \mathbf{r}_{ij}(t)} dA' \right\rangle. \end{aligned} \quad (25)$$

The summations and integrations are freely interchanged here.

Writing out $K(\tau)$ in full, we have

$$\begin{aligned} K(\tau) &= \sum_{i,j} \left\langle \int_A e^{i[(\mathbf{q} + \delta\mathbf{k}) \cdot \mathbf{r}_{ij}(t)]} dA' \right. \\ &\quad \left. \times \sum_{l,m} \int_A e^{-i(\mathbf{q} + \delta\mathbf{k}) \cdot [\mathbf{r}_{lm}(t) + (\delta\mathbf{r}_{lm}(\tau))] } dA' \right\rangle. \end{aligned} \quad (26)$$

Remember that each little area element dA on the face of the photodetector has a different $\delta\mathbf{k}$ associated with it. This fact will be used when we come to evaluate this integral in two spatial cases: a square and a circular photodetector.

Because the particles have random positions at all times, the ensemble average implied by the brackets, will give zero contribution to Q unless $i = j$ and in that case, $\mathbf{r}_{ij}(t) = 0$. Thus $Q = NA$ and

$$Q^2 = N^2 A^2. \quad (27)$$

For $K(\tau)$, we have no such simplification. Every term in Eq. (26) not involving $\delta\mathbf{k}$ can be taken out of the integral, so that this equation can be written in full as

$$K(\tau) = \sum_{i,j,l,m} \langle e^{i\mathbf{q} \cdot (\delta\mathbf{r}_l(\tau) - \delta\mathbf{r}_m(\tau))} e^{-i\mathbf{q} \cdot (\mathbf{r}_j - \mathbf{r}_i + \mathbf{r}_l - \mathbf{r}_m)} B_{lm} C_{ij} \rangle, \quad (28)$$

where, for any i and j

$$C_{ij} = \int_A e^{i\delta\mathbf{k} \cdot \mathbf{r}_{ij}} dA' = C_{ji}^* \quad (29)$$

and

$$B_{lm} = \int_A e^{i\delta\mathbf{k} \cdot (\mathbf{r}_{lm}(t) + \delta\mathbf{r}_{lm}(\tau))} dA'. \quad (30)$$

For every particle pair, the relative change in the particle positions $\delta\mathbf{r}_{lm}(\tau)$ is small compared to their separation $\mathbf{r}_{lm}(t)$, so we can set $C_{lm} = B_{lm}$. Also, the randomness of the particle positions again allows us to simplify the expressions; the only terms in Eq. (28) that will not average to zero are those for which $i = j$ and $l = m$ or $i = l$ and $j = m$. For these terms $(\mathbf{r}_j - \mathbf{r}_i + \mathbf{r}_l - \mathbf{r}_m)$ in Eq. (28) is zero.

Because N is typically very large, we can neglect the N terms for which $i = j = l = m$, there being only N of these terms compared to the $N(N-1) \approx N^2$ particle pairs that do not satisfy this fourfold equality. Taking advantage of this fact, we write

$$K(\tau) = N^2 A^2 + \sum_{l,m \neq l} \langle e^{i\mathbf{q} \cdot [\delta\mathbf{r}_l(\tau) - \delta\mathbf{r}_m(\tau)]} C_{lm} C_{lm}^* \rangle. \quad (31)$$

The first term on the right comes from setting $i = j$ and $l = m$. Particles undergoing Brownian motion are uncorrelated, so we can write

$$\begin{aligned} K(\tau) &= N^2 A^2 + N^2 \langle e^{i\mathbf{q} \cdot \delta\mathbf{r}_{lm}(\tau)} C_{lm} C_{lm}^* \rangle \\ &= N^2 A^2 + N^2 \langle C_{lm} C_{lm}^* \rangle \langle e^{i\mathbf{q} \cdot \delta\mathbf{r}_{lm}(\tau)} \rangle. \end{aligned} \quad (32)$$

We are justified in averaging the product $C_{lm} C_{lm}^* = |C_{lm}|^2$ separately from the remaining phase factor term, because the change in separation $\delta\mathbf{r}_{ij}(\tau)$ in the interval τ has nothing to do with the initial (random) separation $\mathbf{r}_{ij}(t)$ of the Brownian particles. This major simplification is lost when the particles are moving coherently, as discussed in Sec. V for fluid flow.

In the present notation, for any l

$$\langle e^{\pm i\mathbf{q} \cdot \delta\mathbf{r}_l(\tau)} \rangle = e^{-Dq^2\tau}, \quad (33)$$

and the independence of the motion of the particles permits us to write

$$\langle e^{i\mathbf{q} \cdot \delta\mathbf{r}_{lm}(\tau)} \rangle = \langle e^{i\mathbf{q} \cdot \delta\mathbf{r}_l(\tau)} \rangle \langle e^{-i\mathbf{q} \cdot \delta\mathbf{r}_m(\tau)} \rangle. \quad (34)$$

Thus

$$K(\tau) = N^2 A^2 + N^2 \langle |C_{lm}|^2 \rangle e^{-2Dq^2\tau}. \quad (35)$$

Dividing by $Q^2 = N^2 A^2$ from Eq. (28) gives the result we seek for the case of (uncorrelated) Brownian motion of particles in the sample:

$$g(\tau) = 1 + f(A) e^{-2Dq^2\tau}, \quad (36)$$

where $f(A) = \langle |C_{lm}|^2 \rangle / A^2$.

The function C_{lm} depends on the particle separations r_{lm} , and for all applications of interest, we can treat this separation as a continuous variable. Then C_{lm} can be replaced by $C(\mathbf{r})$ where \mathbf{r} is the *separation* of pairs of diffusing particles. We must integrate over all \mathbf{r} lying in the sample volume. In addition, there is an integration over the face x' , y' of the photodetector (see Fig. 5). For algebraic simplicity, we consider the special case of the incident laser beam \mathbf{k}_i traveling along the y axis and illuminating the Brownian particles over the vertical distance $0 \leq y \leq L$. In the integration over the illuminated sample volume, account must be taken of the fact that there is a larger likelihood of finding a pair of particles separated by a short distance y , compared to the probability of encountering particles of separation slightly smaller than L . Because the illuminated region is a thin vertical line (see Fig. 5), the normalized probability density function $w(y)$ has a particularly simple form $w(y) = (2/L) \times (1 - y/L)$ for a light source of length L .^{12,13} The reader is reminded that y is a component of the separation of a pair of particles and not the coordinate y in Fig. 5. In this case $C(\mathbf{r})$ is real and $\langle C(\mathbf{r}) C^*(\mathbf{r}) \rangle = \int_0^L w(y) C(y)^2 dy$.

Before proceeding to the final integration that yields $g(\tau)$, we simplify the exponent $\delta\mathbf{k} \cdot \mathbf{r}$ in the expression for $C(\mathbf{r})$ in Eq. (26). Assuming that the detector is square, has an area

$h \times h$, and its face is normal to the direction of $\langle \mathbf{k}_s \rangle$, the scalar product in Eq. (24) is $\delta \mathbf{k} \cdot \mathbf{r} = k_0 y y' / R$. Then

$$C(\mathbf{r}) = h \int_{-h/2}^{h/2} e^{ik_0 y y' / R} dy' = \frac{h^2 \sin(k_0 h y)}{k_0 h y} = h^2 \text{sinc}(k_0 h y). \quad (37)$$

We use Eq. (37) and the fact that $Q^2 = N^2 h^4$, because the square photodetector has sides h , we have

$$f(A) = \int_0^L (2/L)(1 - y/L) \text{sinc}^2(k_0 y h / R) dy. \quad (38)$$

It has been implicitly assumed in the above calculation that the incident laser beam has a square profile. In reality, laser beams usually have radially Gaussian intensity variation. This fact does not alter the above derivation as long as the beam length L seen by the photodetector is long compared to the Gaussian beam radius.

Consider next the case where the aperture in front of the photodetector is circular with diameter a . Again the incident laser beam is a thin line of light traveling along the y -axis in Fig. 5. We switch to cylindrical coordinates, $\delta \mathbf{k}_s \cdot \mathbf{r} = k_0 r_y y' / R$, where r_y is the component of source coordinate r in the y direction. Taking a to be the diameter of the detector, we obtain

$$\begin{aligned} C(r) &= C(r_y) = \int_0^{a/2} \int_0^{2\pi} e^{i(k_0 r_y r' / R) \cos \phi} d\phi dr_y \\ &= 2\pi \int_0^{a/2} J_0 \left[\frac{k_0 r_y r'}{R} \right] r' dr', \end{aligned} \quad (39)$$

where $J_n(u)$ is a Bessel function of order n . Using $\int_0^u J_0(u') u' du' = u J_1(u)$, we find

$$\begin{aligned} G(\tau) &= 4 \int_0^L (2/L)(1 - r_y/L) \\ &\quad \times [J_1(k_0 a r_y / 2R) / (k_0 a r_y / 2R)]^2 dr_y e^{-2Dq^2 \tau} \\ &= f(A) e^{-2Dq^2 \tau}. \end{aligned} \quad (40)$$

Again, $f(A)$ falls below unity when B is no longer small, because the photodetector is accepting light from many independently fluctuating speckles (intensity maxima), which tend to average out the intensity fluctuations.

V. FLUID FLOW

We now ignore the effect of Brownian motion and instead calculate $G(\tau)$ under conditions where the velocity is changing from point to point and is a function of time t . The above derivation requires surprisingly little modification, even though the functional form of $G(\tau)$ will be entirely different when the particles in the flow are not moving independently. The calculation will show that $G(\tau)$ decays in a time τ_c governed by the velocity variation measured across L . Let $V(L)$ be the rms velocity *difference* across the source width L . We will find that $\tau_c \approx (qV(L))^{-1}$ if $B \ll 1$. If, on the other hand, the photodetector collects light from many speckles, the shape of $G(\tau)$ will be altered.

Again focus attention on a pair of particles, l and m , moving at velocities $\mathbf{v}_l(t)$ and $\mathbf{v}_m(t)$. We can replace $\delta \mathbf{r}_{ij}(\tau)$, the relative change in position of this particle pair in a time τ , by

$$\mathbf{V}_{lm} \tau = \int_t^{t+\tau} [\mathbf{v}_l(t') - \mathbf{v}_m(t')] dt'. \quad (41)$$

We have used the fact that in the short time τ where $G(\tau)$ is appreciable, the change in velocity difference V_{lm} is almost constant. If the flow is turbulent, V_{lm} is a random variable as measured in an experiment that spans many correlation times in the measuring time T .

With this change, the above results can be used, except for the fact that the factorization in Eq. (32) is no longer permissible. Therefore we have

$$K(\tau) = N^2 A^2 + \sum_{i,j,i \neq j} \langle e^{i\mathbf{q} \cdot \mathbf{V}_{ij} \tau} C_{ij} C_{ij}^* \rangle. \quad (42)$$

Here there is no justification for averaging the factor $C_{ij} C_{ij}^*$ separately. To understand this point, consider a pair of particles that are near each other in the source and another pair that is widely separated. There will be a coherence factor B associated with each of these pairs, because closely spaced particles will produce a broader speckle than those that are not, just as a narrow slit produces a broader diffraction maximum than does a wide slit. Thus, the widely spaced pair will receive a smaller weight in $G(\tau)$. It is therefore necessary to assure that $B = hL/R\lambda \ll 1$ if the measurements are to have a reasonably direct interpretation. Reference 13 discusses a calculation and a measurement of the effect on $G(\tau)$ when B is not small, so that the photodetector collects light from many speckles.

As before, the seeding density of the particles is assumed to be sufficiently high that \mathbf{V}_{ij} can be replaced by $\mathbf{V}(\mathbf{r})$, where \mathbf{r} is the distance between a particle pair. Because $\mathbf{V}(\mathbf{r})$ is a random variable that generally will not be Gaussian, the probability distribution P must be left as an unknown function to be determined by the experiment. Let $V_q(r)$ be the component of the velocity difference \mathbf{V} along \mathbf{q} . We will see that the measured $G(\tau)$ is closely related to the Fourier transform of $P(V_q)$. [If light is carried from the sample to the photodetector by single-mode optical fibers, no integral over A is required, and $G(\tau)$ and $P(V_q)$ are cosine transform pairs.²³]

By repeating the same steps needed to obtain $G(\tau)$ for Brownian motion, we calculate that for a source in the form of a thin line of length L and for a scattering angle of 90° ,

$$\begin{aligned} G(\tau) &= \frac{1}{A^2} \int_{V_q(r)=-\infty}^{V_q=-\infty} \int_0^L w(r) P(V_q, r) \\ &\quad \times \cos(qV_q \tau) |C(r)|^2 dV_q(r) dr. \end{aligned} \quad (43)$$

In Eq. (43) the exponential factor in Eq. (42) has been replaced by the cosine, because $K(\tau)$ is real.

For a photodetector with a square face of area $h \times h$,

$$\begin{aligned} G(\tau) &= \int_0^L \int_{V_q} (2/L)(1 - y/L) P(V_q, r) \cos(qV_q \tau) \\ &\quad \times [\text{sinc}(k_0 h r_y / 2R)]^2 dV_q(r). \end{aligned} \quad (44)$$

For laminar flows V_q is not a random variable and no integration over dV_q is necessary. For turbulent flows it has

not been possible to derive $P(V_q, r)$, even when the turbulence is isotropic. For this reason the subject of turbulence remains a very active one,²⁴ to which the photon correlation technique can be employed to advantage.

For a simple example of a laminar flow that is easily studied, consider the seeded sample to be cylindrical in shape and rotating about its axis on, say a record turntable. Let its angular frequency be ω , so that the azimuthal velocity is given by $v_\phi = r\omega$. To avoid having to take into account Brownian motion of the seed particles, one might want to choose a solvent having a large viscosity, such as a mixture of glycerine and water. This choice will make D small, so that the decay term $e^{-2Dq^2\tau}$ can be ignored. If parameters are chosen to assure $B \ll 1$, so that the factors $C(\mathbf{r})$ can be ignored as well, a simple integration of Eq. (43) establishes that

$$g(\tau) = 1 + [\text{sinc}(x)]^2, \quad (45)$$

where $x = qV_q\tau/2 = k_0L\omega\tau/2$. The decaying oscillations of this function are easily observed.

VI. CONCLUSION

Dynamic light scattering has long been a powerful tool for studying a wide range of phenomena, only a few of which have been discussed here. In these and many other applications, the scattering is generated by small particles that have been introduced into a solvent, which is assumed to scatter light weakly. But many fluid-like and glassy systems, such as gels, strongly scatter light by themselves, so that no probe particles need be introduced. The experiments suggested here could easily provide a launching point for original investigations.

No mention has been made of the use of optical fibers to couple the light from the source to the photodetector. With this new technical development, dynamic light scattering experiments become much more convenient. Because single-mode fibers will conduct light having a single wavenumber, we can satisfy the coherence condition $B \ll 1$ without having to put the photodetector and sample far from each other. A useful introduction to this technique can be found in recent work by Du *et al.*²³ The measurements shown in Fig. 3 were made with a relatively inexpensive optical fiber that did not preserve polarization.

ACKNOWLEDGMENTS

I am especially indebted to P. Tong, K. J. Måløy, and J. R. Cressman for their contribution to my understanding of this subject and to Rob Cressman and Quentin Bailey for their careful reading of this paper. This work is supported by grants from the NSF and NASA.

¹For example, older models of Malvern, Langley Ford, and Brookhaven correlators should work fine.

²A good source of such particles is PolyScience, 6600 W. Touhy Ave., P.O. Box 48312, Niles, IL 60714.

³D. Halliday, R. Resnick, and J. Walker, *Fundamentals of Physics* (Wiley, New York, 1997), 5th ed., Chap. 37.

⁴C. Kittel, *Elementary Statistical Physics* (Wiley, New York, 1958).

⁵F. Reif, *Fundamentals of Statistical and Thermal Physics* (McGraw-Hill, New York, 1965).

⁶A. Einstein, in *Investigations on the Theory of Brownian Motion*, edited by R. Furth and A. D. Cowper (Dover, New York, 1956), Chap. I.

⁷B. J. Berne and R. Pecora, *Dynamic Light Scattering* (Wiley-Interscience, New York, 1976).

⁸W. I. Goldburg, "The dynamics of phase separation near the critical point: spinodal decomposition and nucleation," in *Scattering Techniques Applied to Supramolecular and Nonequilibrium Systems*, edited by S.-H. Chen, B. Chu, and R. Nossal (Plenum, New York, 1981), pp. 383–409, and other articles in this volume.

⁹L. Mandel and E. Wolf, "Coherence Properties of Optical Fields," *Rev. Mod. Phys.* **37**, 231–287 (1965).

¹⁰R. Hanbury Brown and R. Q. Twiss, "Correlation between photons in two coherent beams of light," *Nature (London)* **177**, 27–29 (1956).

¹¹Edmund Scientific in Barrington, NJ is a good source for interference filters and other optical components.

¹²P. Tong *et al.*, "Turbulent transition by photon-correlation spectroscopy," *Phys. Rev. A* **37**, 2125–2133 (1988).

¹³K. J. Måløy *et al.*, "Spatial coherence of homodyne light scattering from particles in a convective velocity field," *Phys. Rev. A* **46**, 3288–3291 (1992).

¹⁴H. Kellay *et al.*, "Experiments with Turbulent Soap Films," *Phys. Rev. A* **74**, 3975–3978 (1995).

¹⁵Also called 2,6-dimethylpyridine.

¹⁶H. E. Stanley, *Introduction to Phase Transitions and Critical Phenomena* (Oxford, New York, 1971).

¹⁷W. I. Goldburg, "Light scattering investigations of the critical region in fluids," in *Light Scattering Near Phase Transitions*, edited by H. Z. Cummins and A. P. Levanyuk (North-Holland, New York, 1983), pp. 531–581; J. D. Gunton, M. San Miguel, and P. S. Sahni, *Phase Transitions and Critical Phenomena*, edited by C. Domb and J. L. Lebowitz (Academic, London, 1983), Vol. 8.

¹⁸H. C. Van de Hulst, *Light Scattering by Small Particles* (Wiley, New York, 1957).

¹⁹J. D. Jackson, *Classical Electrodynamics* (Wiley, New York, 1992), 2nd ed.

²⁰N. Clark, J. H. Lunacek, and G. B. Benedek, "A study of Brownian motion using light scattering," *Am. J. Phys.* **38**, 575–585 (1970).

²¹C. L. Mehta, "Coherence and statistics of radiation," in *Lectures in Theoretical Physics*, Vol. 7C, edited by Wesley E. Brettin (University of Colorado, Colorado, 1965), pp. 345–401.

²²B. Chu, *Laser Light Scattering* (Academic, New York, 1991), 2nd ed., Chap. VII.

²³Y. Du, B. J. Ackerson, and P. Tong, "Velocity difference measurement with a fiber-optic coupler," *J. Opt. Soc. Am. A* **15**, 2433–2439 (1998).

²⁴U. Frisch, *Turbulence, the Legacy of A. N. Kolmogorov* (Cambridge U. P., New York, 1995).